DURABILITY ASSESSMENT OF VARIOUS GAMMA TIAL ALLOYS

Brad Lerch,[1] Sue Draper,[1] Mike Pereira,[1] and Wyman Zhuang[2]

[1]National Aeronautics and Space Administration, Glenn Research Center; 21000 Brookpark Road; Cleveland, OH 44135, USA
[2]Aeronautical and Maritime Research Laboratory; Melbourne, Victoria, 3207, Australia

Abstract

Seven cast and one wrought γ-alloys were ballistically impacted and tested under high cycle fatigue. The fatigue strength of each alloy was characterized as a function of initial flaw size and modeled using a threshold-based fracture mechanics approach.

Introduction

Emerging families of alloys based on γ-TiAl have recently been developed for aerospace applications. Their advantage is their low density (3.8 g/cm^3) coupled with good high temperature properties. The specific strength makes the alloys attractive for rotating components such as low pressure turbine (LPT) and compressor blades in aircraft engines. As part of this effort, the authors have been investigating the impact durability of γ-TiAl alloys since 1995. The approach was to impact a series of γ-TiAl alloys, relate the various impact parameters to initial surface cracks and assess the residual high cycle fatigue (HCF) strength of these materials. The initial work was performed on cast Ti-48Al-2Cr-2Nb (Ti-48-2-2; a/o) in collaboration with General Electric Aircraft Engines (GEAE) and was aimed at an LPT application. Subsequent work defined the acceptable design limitations associated with impact damage on Ti-48-2-2. Impact studies were expanded to include several different cast TiAl alloys. These alloys resulted in a more complete understanding of alloy effects on impact and fatigue properties. In addition, a wrought TiAl alloy was investigated. This publication is a summary of the fatigue results from this work. Due to space limitations, only selected examples are given, but a complete set of the data can be found in reference 1.

Materials

Eight materials were used in this study and are designated as follows: Ti-48-2-2, GEAE Ti-47-2-2, Howmet 47-2-2, CMU 47-2-2, ABB-2, ABB-23, NCG359E, and 95A. Chemistries for these alloys can be found in reference 1. Specimens for Ti-48-2-2 and the ABB-2 materials were cast-to-size in a dog-bone configuration. These flat specimens had gage sections which were reduced in both the width and thickness dimensions with elliptical cross sections 25 by 3.7 mm, respectively. The cast-to-size sample edges simulated the leading edges of actual LPT airfoils by duplicating the leading edge radii and neighboring curvature of a LPT blade. Since the cost and difficulty of casting these specimens would inhibit the progress in studying the impact resistance of additional alloys, all of the other specimens were machined from plates. A sample design was utilized which was similar to the cast-to-size samples, albeit smaller in dimensions. The machined samples also contained an elliptical gage cross section of dimensions 9.9 by 1.9 mm.

The cast-to-size Ti-48-2-2 represented the baseline material. Since the Al content varies slightly from casting to casting, and the strength and ductility of Ti-48AL-2Cr-2Nb varies with Al content [2] the effect of low Al on the impact resistance of Ti-48-2-2 was of interest. To this end, plates of a lower Al alloy (Ti-47-2-2) were obtained from GEAE (47.1 a/o) and still lower Al containing alloys from Howmet (46.4 a/o) and Carnegie Mellon University, CMU (46.5 a/o). The cast-to-size ABB-2 specimens (an alloy from ALSTOM POWER, CH, Ltd.) were provided by Howmet, Inc. ABB-2 has a higher strength and lower ductility than Ti-48-2-2. A few specimens of ABB-23 were also available from ALSTOM POWER, CH, Ltd. ABB-23 has boron added for grain refinement. NCG395E is a cast TiAl alloy developed by GEAE. This Ta-containing alloy has a higher strength than Ti-48-2-2. The impact resistance of a wrought alloy was also of interest to study the effect of a more refined, uniform microstructure typical of wrought alloys. Wrought alloys have a potential use as compressor blades. The alloy chosen was alloy 95A, a version of the Air Force's K5 alloy. Y.W. Kim of UES, Inc., Dayton, Ohio, supplied a forged pancake of 95A from which samples were machined.

Experimental Procedure

Specimens were impacted with a ballistic impact rig that consists of a precision gun barrel mounted on a load frame with an attached furnace. The gun barrel was aimed perpendicular to the width of the specimen and the intended impact site was 4 mm away from the leading edge. The projectiles were either 1.6- or 3.2-mm-diameter ball bearings and chosen to cover a wide range of expected debris in an engine. The specimens were impacted at 260 °C in air under a tensile load of 70 MPa. After impact, the specimens were examined in a scanning electron microscope (SEM). Crack lengths were measured on both the front and back sides. The front side cracks are termed Hertzian (HZ), since they are similar in appearance to the Hertzian cracks found in glass. The cracks on the opposite side of the sample are perpendicular to the specimen axis and termed Back Side (BS) cracks. The BS cracks form as a result of the tensile stresses resulting from impact.

As-received and impacted samples were tested in high-cycle fatigue (HCF) at 650 °C at a frequency of 100 Hz. The fatigue crack growth rate is highest for Ti-48Al-2Nb-2Cr at 650 °C [3], and therefore this temperature was chosen for testing to simulate the worst-case scenario. All the other alloys were tested at 650 °C for comparison. A few tests were conducted at 730 °C on ABB-2, since this was a potential service temperature for the material. A load ratio, R, of 0.05 ($R = \sigma_{min}/\sigma_{max}$, the ratio of minimum to maximum applied stress) was used in all experiments. Due to the flat nature of the S-N (stress versus cycles to failure) curve for

γ-TiAl, step tests [4,5] were used to determine the fatigue strength. In the step tests a block size of 10^6 cycles was utilized, although 10^7 was also used on selected Ti-48-2-2 samples to see if block size had an influence—none was observed. If the sample survived the block, then the maximum stress level was increased by approximately 14 MPa. It should be noted that a potential drawback to such testing is the possibility of coaxing, which would lead to fatigue strengths that were meaningless for design. Coaxing is an artificially high-fatigue-limit strength that results from step testing rather than conventional single stress limit-to-failure procedures [6]. Coaxing was investigated as part of another study [7] and shown to not occur in these tests.

Results and Discussion

A summary of the microstructures for each alloy is given in table I. The cast-to-size Ti-48-2-2 samples and the cast Ti-47-2-2 plates had duplex microstructures. The Ti-48-2-2 samples had approximately 61 percent gamma grains with an average grain size of 64 μm. The GEAE and the CMU Ti-47-2-2 plates had similar microstructures with 65 percent lamellar grains and gamma grains with average diameters between 58 and 60 μm. However, the Ti-47-2-2 plates purchased from Howmet had a non-uniform microstructure. The edges of the plates had a nearly fully lamellar microstructure with columnar colony grains but the center of the plates had a more duplex microstructure with a bimodal distribution of gamma grains. The NCG359E plates also

had a duplex microstructure with 32 percent gamma grains with an average grain size of 69 μm. The cast-to-size ABB-2 samples had a non-uniform microstructure with columnar lamellar colonies at the edge and a more duplex microstructure at the center of the samples. The addition of boron in the ABB-23 resulted in a refined lamellar microstructure with lamellar grain sizes averaging 59 μm. The only wrought alloy investigated, 95A, had a thermomechanically treated lamellar microstructure with a lamellar colony size averaging 288 μm.

The tensile properties of the various alloys are given in table II. The cast and machined Ti-48-2-2 room temperature tensile data were supplied by GEAE, and ALSTOM Power supplied the ABB-23 data due to a lack of excess material to make tensile specimens. The cast-to-size Ti-48-2-2 had the lowest tensile strength but the highest ductility with an average 0.2 percent offset yield strength (0.2%YS) of 326 MPa, an average ultimate tensile strength (UTS) of 422 MPa, and a plastic elongation of 1.7 percent, all at 25 °C. The cast Ti-47-2-2 plates supplied by GEAE, Howmet, and CMU had higher strengths but lower ductilities. Their average room temperature properties were: YS 450 MPa, UTS 520 MPa, and plastic elongations 1.2 percent. The NCG359E plate had very similar tensile properties to the Ti-47-2-2 plates. The ABB-2 and ABB-23 had nearly identical tensile properties to one another and both had higher strengths and lower ductilities compared to the other alloys.

Table I.—γ-TiAl alloy microstructure

Alloy	Lamellar volume fraction	Gamma grain size, μm	Lamellar colony size, μm
Cast-to-size Ti-48-2-2	0.39 ± 0.06	64.0 ± 2.3	
GEAE Ti-47-2-2	0.65 ± 0.04	60.3 ± 3.3	
CMU Ti-47-2-2	0.65 ± 0.04	58.2 ± 4.4	
Howmet Ti-47-2-2	Non-uniform but nearly lamellar	Irregular, bimodal	Large, columnar colonies near edge
Cast-to-size ABB-2	Variable. Nearly fully lamellar near edge, duplex in center	Irregular	Large, columnar colonies near edge
ABB-23	~1		58.5 ± 3.2
NCG359E	0.68 ± 0.11	69.4 ± 7.1	
95A	~1		288 ± 21.4

Table II.—Average tensile properties for γ-TiAl alloys

Alloy	Temperature, °C	Yield strength, MPa	Tensile strength, MPa	Elongation, %	Elastic modulus, GPa
Cast-to-size Ti-48-2-2	23	326	422	1.70	168
	650	284	474	5.10	141
GEAE Ti-47-2-2	23	458	536	1.42	172
	650	--	--	--	--
CMU Ti-47-2-2	23	433	499	1.00	187
	650	359	552	4.10	166
Howmet Ti-47-2-2	23	449	516	.99	151
	650	353	526	2.76	128
Cast-to-size ABB–2	23	504	599	0.89	173
	650	413	571	1.97	147
ABB–23	23	528	589	0.58	189
	650	440	532	1.07	156
NCG359E	23	422	482	1.01	161
	650	359	524	3.65	171
95A	23	417	547	1.12	149
	650	331	587	3.93	146

This section addresses the fatigue properties of the various γ-alloys. Both virgin and impacted samples were cycled under HCF conditions at elevated temperatures. The main thrust of this section is to assess the contribution of defects on the fatigue strength. Cracks caused by the impacts are examined as well as other inherent flaws in the samples, such as casting defects. These effects are modeled using a conventional LEFM (linear elastic fracture mechanics) approach. The fatigue properties are related to various alloy specific properties.

Figure 1 is an S-N curve for the various γ-TiAl alloys studied. The data for this curve were taken from virgin samples either defect-free or containing defects having an area less than 0.1 mm²—a size which ostensibly had no influence on fatigue strength. Note that of the data points representing the 50 samples in figure 1, only 12 of the points represent samples with observable defects. In general, the data fall into one grouping with fatigue stresses at a life of 10,000 cycles ranging from approximately 290 to 390 MPa. Endurance limits (at 10⁶) from conventional, single-stress fatigue tests are given by Wright et al. [8] as 335 MPa for cast Ti-48-2-2 and by Recina and Karlsson [9] as 325 MPa for cast ABB-2 and these values are consistent with our data. Two alloys seem to have superior fatigue properties: CMU 47-2-2 and ABB-23. At a life of 10,000 cycles ABB-23 has a fatigue strength of approximately 470 MPa, the CMU 47-2-2 alloy has a fatigue strength of 400 MPa. Note that the enhancement in fatigue strength of these two alloys is not necessarily a consequence of their respective tensile properties (table II), since the other alloys have similar or better properties. Nor is there any obvious correlation with either

chemistry or microstructure. These variables interact and may have conflicting influences on the fatigue strength. Note that this investigation was not a designed study to assess the effects of these variables on fatigue strength. Figure 1 was an afterthought and was meant only to provide a more conventional look at the data.

Another observation can be made in figure 1. Of the 50 data points in this figure, only 7 of the samples lasted longer in the final step than 25,000 cycles. It can be implied that during the step tests the crack grows rapidly once the threshold stress value is reached. This is consistent with observations on impacted samples in both this study and others [10, 11] where the specimen fails in the last step in a limited number of cycles. Nicholas [11] has shown for Ti-6Al-4V that precracked samples failed during step testing early in the last step and attributed this to a well-defined threshold and the lack of importance of an initiation phase. He continued to show that uncracked samples failed at a more random cycle number indicating that the initiation phase for these samples was both random and dominant to the life. By applying the conclusions of Nicholas [11] to figure 1, we believe that the majority of the cast γ-TiAl alloys have sufficient, available initiation mechanisms—whether it is some small casting or machining defect, a lamella oriented for easy crack initiation, or some unknown microstructural anomaly—such that initiation has already happened or can easily occur, and the bulk of the life in the last step is therefore propagation controlled and relatively constant.
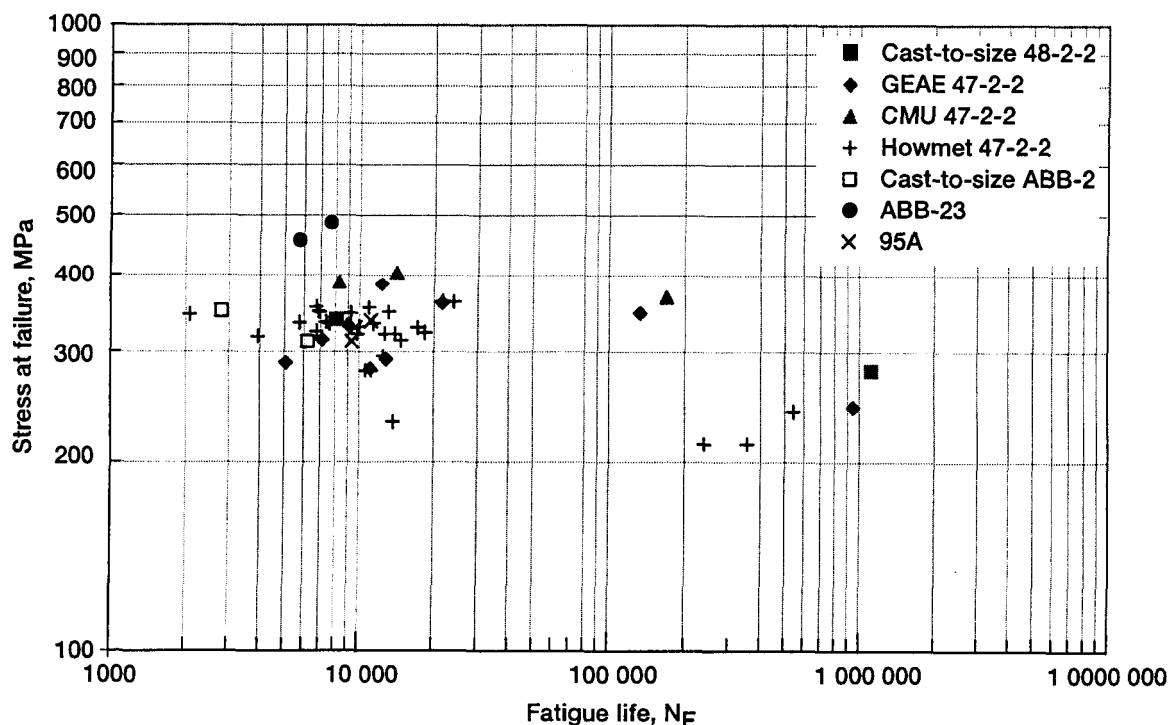

Figure 1.—Fatigue life curve of γ-alloys tested at 650 °C and a load ratio of 0.05.

The fatigue strength calculated from fracture mechanics was plotted against the measured fatigue strength at threshold to gauge the applicability of this approach for predicting life. To calculate the fatigue strength, the following equation was used

$$\Delta\sigma = \frac{\Delta K_{th}}{F(a/w)} \cdot \sqrt{\pi a} \qquad (1)$$

where $\Delta\sigma$ is the predicted fatigue strength range for the block size, ΔK_{th} is the stress intensity range at the threshold, $F(a/w)$ is a geometry correction factor, and a is the defect length. Since the load ratio for these tests was approximately zero (i.e., R = 0.05), the deltas on σ and K will henceforth be dropped. Note that K_{th} was unavailable for these alloys. It would have been ideal to have this information on the exact lots of material used in this study. However, this was beyond the scope of the current study. There are some values for K_{th} in the literature for similar alloys and these were used for comparison and discussed later in this report. Given the lack of threshold values, we chose to back-calculate them from an iterative process, trying various values for K_{th} until a visual good fit with the data was obtained. This method was adequate since we had various defect types which covered a wide range of flaw sizes.

Various stress intensity solutions were assumed for the defects observed in this work. For BS cracks, a corner crack solution as given by Newman and Raju [12] was used. However, as the crack depth increased or the BS crack approached the edge of the sample (and this happened for the CMU Ti-47-2-2, ABB-2, and 95A materials), the BS crack was better represented by a SEN solution [13]. HZ cracks looked most like an edge crack having a different crack length at the front and the back surface [14]. It was found that using the smaller crack length (i.e., the length on the impacted side) gave the best fit of the data. The inclination of the HZ crack, which would introduce mixed-mode loading, was not taken into account in the modeling. Pores were approximated using an embedded crack solution [12]. Occasionally, cracks initiated at surface defects (face defects) either due to machining or from casting defects. These were approximated using a surface crack solution [12].

Fatigue strength predictions are shown for the cast-to-size Ti-48-2-2 in figure 2. Similar plots for the remaining alloys can be found in ref. 1. A K_{th} value of 8.8 MPa $\sqrt{m}$ was found to best fit the Ti-48-2-2 data for all of the defect types. There was a number of the porosity containing samples whose data are over-predicted. This is a result of an inaccuracy in measuring the defect size. For example, figure 3 is a micrograph of a specimen containing a large area of microshrinkage in the middle of the sample. The solid line outlines the defect size as was used to calculate the point in figure 2. If however, the dashed outline is used, the predicted fatigue strength drops from 386 to 217 MPa and falls very near the prediction line (the arrow tip represents the position of the adjusted point). While this is a large difference in predicted fatigue strength, the difference in defect size (fig. 3) is marginal. Without knowledge of figure 2, either crack outline in figure 3 would seem acceptable.
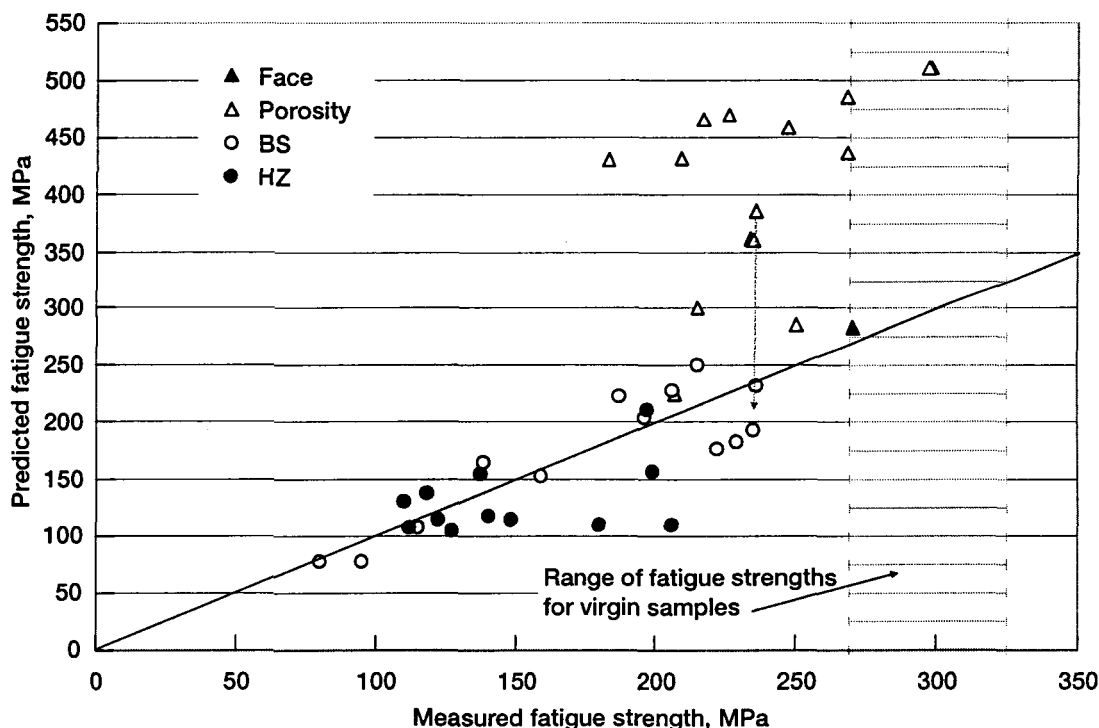

Figure 2.—Prediction capability for cast-to-size Ti-48-2-2 for a ΔK_{th} of 8.8 MPa$\sqrt{m}$.
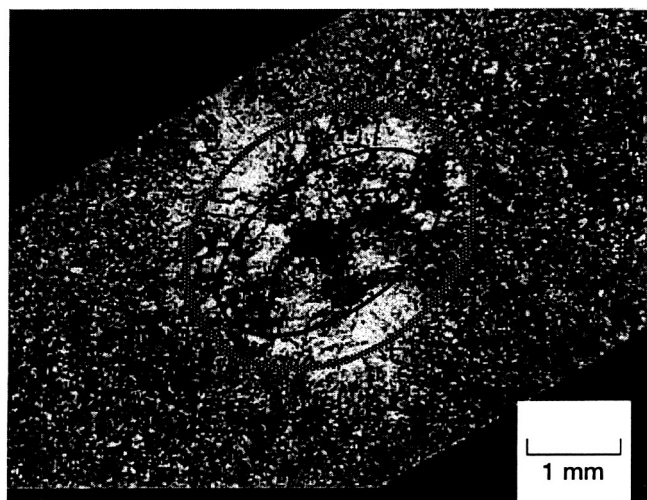
Figure 3.—Extent of microshrinkage used in figure 2.

As the measured fatigue strength increases in figure 2, the prediction line crosses a range of values representing the undamaged samples. These samples have virgin material strengths and represent the fatigue endurance limit corresponding to the block size. This band was determined based only on two defect-free samples and has a range of 58 MPa.

The back-calculated K_{th} values are given in table III along with values taken from the literature. In general K_{th} for this class of alloys is approximately 9 MPa $\sqrt{m}$ and our results compare favorably with these values. There is some variation in the literature values presented in table III. Most of these points were taken at temperatures other than 650 °C and at different frequencies. The actual microstructures may also be different from ours. All of these variables can affect the threshold values.

One area of concern for these alloys is the scatter in the data. An attempt at describing the scatter is given in table IV. In this table the range of scatter as calculated in two different ways is shown, along with the sample size, n. For the virgin samples and reasonable sample sizes, the range of scatter can be as high as 141 MPa. The range of scatter from the flawed samples taken from the fracture mechanics analysis (e.g., fig. 2) is on the order of 90 MPa for reasonable sample sizes. This is not unusually large as many cast aluminum alloys [15] and cast steels [16] have spreads in the fatigue data of 70 to 100 MPa. The scatter in the fatigue endurance limit from conventional fatigue tests on extruded Ti-6Al-4V is 140 MPa [17]. Also, this size of scatter can be ascertained from the data of two groups of researchers on cast gamma alloys [9,18]. While alloys other than the first three alloys

in table IV show lower scatter in their virgin state, they have similar scatter to the first three alloys in the defect-containing state. It is therefore suspected that their small scatter is only a manifestation of the limited sample size. Finally, since 95A is a wrought alloy, it was anticipated that it would exhibit less scatter. There is a limited amount of data on the virgin samples suggesting that they may indeed exhibit less scatter. However, for at least the defect containing samples the scatter is the largest of all the alloys.

γ-TiAl in the lamellar form is susceptible to cleavage fractures. Many researchers [9,19,20] have shown that cracked lamellae occur during cyclic loading and that this susceptibility leads to early crack initiation. Recina and Karlsson [9] suggest that the scatter in fatigue life is partially due to the ease of interlamellar cleavage. Furthermore, Wu et al. [21] postulate that the scatter in low-cycle fatigue (LCF) data is a direct consequence of the initial size of the cleavage crack (i.e., the lamellae colony size). Given the large colony sizes of most of the alloys used in this study, the observed scatter is to be expected. The ABB-23 alloy has the smallest lamellae colony size and appears to have the smallest scatter in table IV. This alloy also had the highest tensile and fatigue strengths, and one of the highest K_{th}.

Per the suggestions of Bowen [22] and Recina and Karlsson [9], and consistent with the results shown here, reducing the lamellar colony size should reduce fatigue scatter and improve the mean strength of these alloys. Recina and Karlsson [9] have gone as far as saying that colonies should be kept to sizes <100 μm. The colony size for the γ-alloys used in this report is generally larger, sometimes an order of magnitude larger than 100 μm. Even if the colony size is smaller than 100 μm, there can be an occasional

Table III.—Fatigue thresholds for various γ-TiAl alloys

Alloy	Fatigue threshold, K_{th}, MPa $\sqrt{m}$	
	This report[a]	Literature values
Cast-to-size 48-2-2	8.8	--
GEAE 47-2-2	8.2	4.5 [8] 6 [23] 6.8 [24]
CMU 47-2-2	12.1	7 [3] 8 [25] 9 [26] 12 [3]
Cast-to-size ABB-2	9.9	8 [27] 8.5 [20]
ABB-23	11.0	9 [27]
NCG359E	11.0	--
95A	11.0	7 [28] 9 [3]

[a]Values were back-calculated using equation (1)

Table IV.—Fatigue scatter for γ-TiAl alloys

Alloy	Virgin samples		Flawed samples	
	Range, MPa	Samples size, n	Range,[a] MPa	Sample size, n
Cast-to-size 48-2-2	58	2	74	28
GEAE 47-2-2	141	9	96	16
Howmet 47-2-2	129	25	--	--
CMU 47-2-2	36	3	89	12
Cast-to-size ABB-2	24	2	63	12
ABB-23	30	2	40	6
NCG359E	--	0	61	7
95A	25	4	101	10

[a]Range is two times the standard error of the regression

lamella of large size or neighboring lamellae of similar orientations which combined can act as one large colony. Therefore, for minimal scatter the lamellar colony size should be uniform and probably on the order of 60 μm (similar to the ABB-23).

For damage tolerant design the use of fracture mechanics was shown to be a useful tool. Given accurate knowledge of the flaw size, the fatigue strength can be easily predicted. This assumes that the fatigue crack threshold, K_{th}, is well-known for the alloy, an assumption that was not realized in this study. Obviously, improvement of the damage tolerance of these alloys would necessitate a larger K_{th}. It is not clear from this study how that would be done. These results suggest that a more refined and uniform grain size seems to be beneficial, as evidenced by both the high K_{th} and the highest virgin fatigue strength of the ABB-23 alloy. Higher tensile ductilities also seem to lead to apparent high K_{th}, perhaps through the additional plastic deformation absorbed at the impact site and the influence of the incurred plasticity on the crack tip. Further investigations are required in this area, as the current study was not initially designed to investigate the relationship between microstructure, tensile and fatigue properties. These relationships were often obscured by conflicting variables. The most significant nuisance variable was the large lamellar colonies in most of the alloys, including the one wrought material. It is therefore recommended that this line of research be pursued further once more refined microstructures are available.

Summary and Conclusions

Seven cast alloys and one wrought alloy were evaluated to assess their ballistic impact resistance. Impacted fatigue specimens were subjected to HCF using the step test method. The amount of degradation in the fatigue strength was measured and predicted using a threshold-based fracture mechanics approach. Back-calculated K_{th} values agreed with published values for similar alloys giving validity to the threshold-based approach. A nuisance variable in this study was the large lamellar colony size, which added to the scatter in the fatigue data. The large colony sizes also obscured the relationship between tensile properties and fatigue resistance. Based on the observations, a lamellar colony size of 60 μm gives good fatigue properties with minimal scatter.

Acknowledgments

References

1. S.L. Draper B.A. Lerch, J.M. Pereira, K. Miyoshi, V.K. Arya, and W. Zhuang, "Durability Assessment of Gamma TiAl–Final Report," NASA/TM—2003-212303.

2. S.L. Draper et al., "The Effect of Ballistic Impacts on the High-Cycle Fatigue Properties of Ti-48Al-2Nb-2Cr (Atomic Percent)," *Metall. Trans.*, 32A, 2001, 2743–58.

3. J.M. Larsen et al., "An Overview of the Structural Capability of Available Gamma Titanium Aluminide Alloys," *Gamma Titanium Aluminides*, eds. Y.W. Kim, R. Wagner and M. Yamaguchi, (Warrendale, PA: TMS, 1995), 821–834.

4. J.A. Collins, *Failure of Materials in Mechanical Design*, (New York, NY: John Wiley & Sons, 1993), 379–381.

5. J. Denk and S. Amhoff, "Determination of the High Cycle Fatigue Strength with a Load-Increasing Single Specimen Technique," *Fatigue '96: Proc. 6th Int. Fatigue Congress*, vol. III, eds. G. Lutjering and H. Nowack (New York, NY: Elsevier Science, Inc., 1996), 1967–72.

6. G.M. Sinclair, "An Investigation of the Coaxing Effect in Fatigue of Metals," *Proc. ASTM*, 52 (1952), 743–758.

7. B.A. Lerch, S.L. Draper, and J.M. Pereira, "Conducting High-Cycle Fatigue Strength Step Tests on Gamma TiAl," *Metall. Trans.*, 33A, 2002, 3871–3874.

8. P.K. Wright et al., "Defect Behavior in Gamma Titanium Aluminides," *Structural Intermetallics 2001*, eds., K.J. Hemker, D.M. Dimiduk, H. Clemens, R. Darolia, H. Inui, J.M. Larsen, V.K. Sikka, M. Thomas and J.D. Whittenberger (Warrendale, PA: TMS, 2001), 315–322.

9. V. Recina and B. Karlsson, "High Temperature Low Cycle Fatigue Properties of Ti-48Al-2W-0.5Si Gamma Titanium Aluminide," *Materials Science and Engineering*, A262, (1999), 70–81.

10. *PRET: A University-Industry Partnership for Research and Transition of Gamma Titanium Aluminides, Annual Report – Sept. 1999* (Report, Carnegie-Mellon University, Pittsburgh, PA, 1999), Chap. 8.

11. T. Nicholas, "Step Loading, Coaxing and Small Crack Thresholds in Ti-6Al-4V under High Cycle Fatigue," *Fatigue – David L. Davidson Symposium*, eds. K.S. Chan, P.K. Liaw, R.S. Bellows, T.C. Zogas, and W.O. Soboyejo, (Warrendale, PA: TMS, 2002), 91–106.

12. J.C. Newman, Jr. and I.S. Raju, "Stress-Intensity Factor Equations for Cracks in Three-Dimensional Finite Bodies," *Fracture Mechanics: Fourteenth Symposium - Volume I: Theory and Analysis, ASTM STP 791*, eds. J.C. Lewis and G. Sines (Philadelphia, PA: ASTM, 1983), I–238–I–265.

13. H. Tada, P.C. Paris, and G.R. Irwin, *The Stress Analysis of Cracks Handbook, 2nd edition*, (St. Louis, MO: Paris Productions, Inc., 1985), 2.10–2.11.

14. *Stress Intensity Factors Handbook, Vol. 2*, ed. Y. Murakami, (New York, NY: Pergamon Press, 1987), 837.

15. "Aluminum Alloys; Cast (AlC-3100)," *Aerospace Structural Metals Handbook, 1997 Edition*, (West Lafayette, IN: CINDAS, Purdue University, 1997).

16. *ASM Handbook #1: Properties and Selection*, (Metals Park, OH: ASM, 1961), 130 and 385.

17. *Mil-Handbook 5G, Metallic Materials and Elements for Aerospace Vehicle Structures*, 1994, 5–68.

18. S.J. Trail and P. Bowen, "Effects of Stress Concentrations on the Fatigue Life of a Gamma-Based Titanium Aluminide," *Materials Science and Engineering*, A192/193, (1995), 427–434.

19. J. Kumpfert, Y.W. Kim, and D.M. Dimiduk, "Effect of Microstructure on Fatigue and Tensile Properties of the Gamma TiAl Alloy Ti-46.5Al-3.0Nb-2.1Cr-0.2W," *Materials Science and Engineering*, A192/193, (1995), 465–473.

20. M. Nazmy et al., "Effect of Surface Defects on the Fatigue Behavior of a Cast TiAl Alloy," *Mat. Res. Soc. Symposium Proc., vol. 646: High-Temperature Ordered Intermetallic Alloys IX*, eds., J.H. Schneibel, K.J. Hemker, R.D. Noebe, S. Hanada, and G. Sauthoff (Warrendale, PA: MRS, 2001), N5.44.1–N5.44.6.

21. X. Wu et al., "Micro-Yield and the Fatigue Limit of TiAl Alloys," *Structural Intermetallics 2001*, eds., K.J. Hemker, D.M. Dimiduk, H. Clemens, R. Darolia, H. Inui, J.M. Larsen, V.K. Sikka, M. Thomas, and J.D. Whittenberger, (Warrendale, PA: TMS, 2001), 289–294.

22. P. Bowen, R.A. Chave, and A.W. James, "Cyclic Crack Growth in Titanium Aluminides," *Materials Science and Engineering*, A192/193 (1995), 443–456.

23. T.S. Harding and J.W. Jones, "Fatigue Thresholds of Cracks Resulting from Impact Damage to γ-TiAl," *Scripta Materialia*, 43 (2000), 623–629.

24. T.S. Harding and J.W. Jones, "The Effect of Impact Damage on the Room-Temperature Fatigue Behavior of γ-TiAl," *Metall. Trans.*, 31A (2000), 1741–1752.

25. K.S. Chan and D.S. Shih, "Fundamental Aspects of Fatigue and Fracture in a TiAl Sheet Alloy," *Metall. Trans.*, 29A (1998), 73–87.

26. J.J. Kruzic, J.P. Campbell, and R.O. Ritchie, "On the Fatigue Behavior of γ-Based Titanium Aluminides: Role of Small Cracks," *Acta Mater.*, 47 (3) (1999), 801–816.

27. V. Lupinc et al., "Creep, Fatigue and Crack Propagation Behavior of a New Industrially Developed γ-TiAl Alloy," *Structural Intermetallics 2001*, eds., K.J. Hemker, D.M. Dimiduk, H. Clemens, R. Darolia, H. Inui, J.M. Larsen, V.K. Sikka, M. Thomas, and J.D. Whittenberger, (Warrendale, PA: TMS, 2001), 709–716.

28. A.H. Rosenberger, B.D. Worth, and S.J. Balsone, "Environmental Effects on the Fatigue Crack Growth of Gamma Titanium Aluminides," *Fatigue '96: Proc. 6th Int. Fatigue Congress*, vol. III, eds. G. Lutjering and H. Nowack (New York, NY: Elsevier Science, Inc., 1996), 1785–1790.

29. T.S. Harding and J.W. Jones, "Effect of Foreign Object Damage on the Fatigue Strength of an XD γ-TiAl Alloy," *Scripta Materialia*, 43 (2000), 631–636.